Supplement of

Glacial-interglacial contrasts in the marine inorganic carbon chemistry of the Benguela Upwelling System

Szabina Karancz[1]; Lennart J. de Nooijer[1]; Bas van der Wagt[1]; Marcel T. J. van der Meer[2], Sambuddha Misra[3]; Rick Hennekam[1]; Zeynep Erdem[2]; Julie Lattaud[4]; Negar Haghipour[5,6]; Stefan Schouten[2,7]; Gert-Jan Reichart[1,7]

[1] Department of Ocean Systems, NIOZ Royal Netherlands Institute for Sea Research, Texel, The Netherlands

[2] Department of Marine Microbiology and Biogeochemistry, NIOZ Royal Netherlands Institute for Sea Research, Texel, The Netherlands

[3] Centre for Earth Sciences, Indian Institute of Science, Bangalore, India

[4] Department of Environmental Sciences, University of Basel, Basel, Switzerland

[5] Geological Institute, Department of Earth Sciences, ETH Zürich, Zürich, Switzerland

[6] Laboratory of Ion Beam Physics, ETH Zürich, Zürich, Switzerland

[7] Department of Earth Sciences, Faculty of Geosciences, Utrecht University, Utrecht, The Netherlands

Correspondence to: Szabina Karancz (szabina.karancz@nioz.nl)

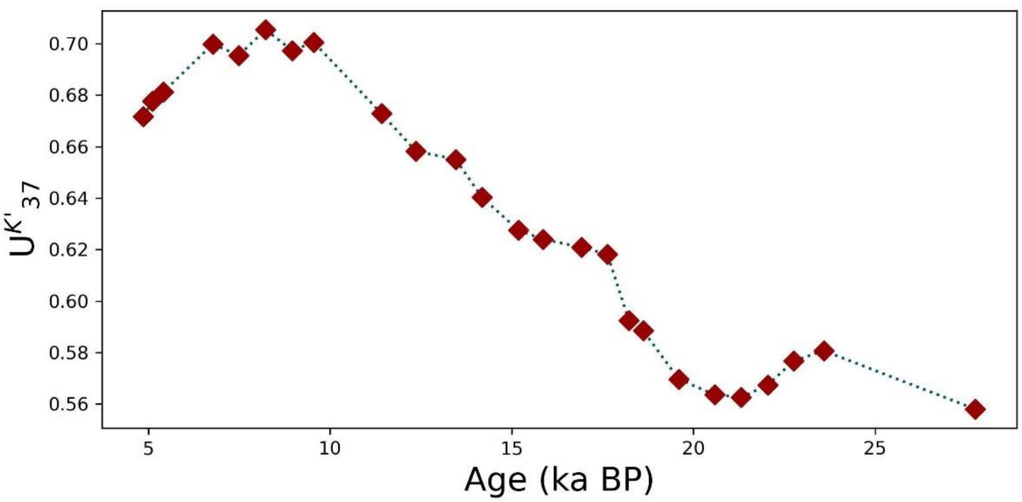

Figure S1. Ketone unsaturation index ($U^{K'}_{37} = C_{37:2} / (C_{37:3} + C_{37:2})$; Prahl and Wakeham, 1987) plotted over the past 27 ka BP.

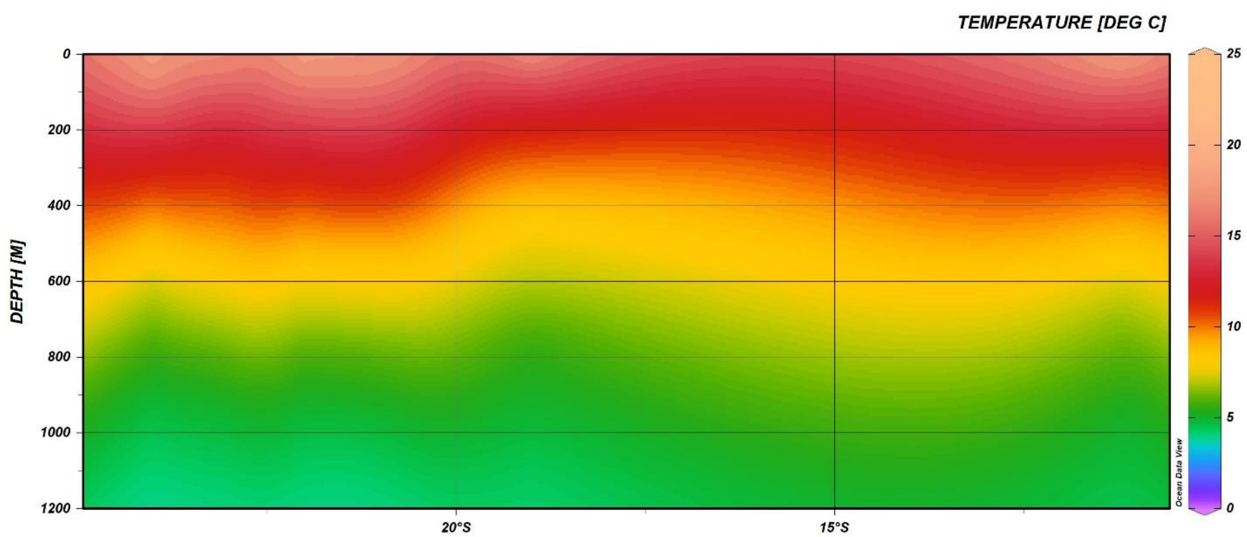

Figure S2. Depth transect in the northern Benguela Upwelling System showing temperature distribution. Temperature values are obtained from GLODAPv2023 (Lauvset et al., 2024).

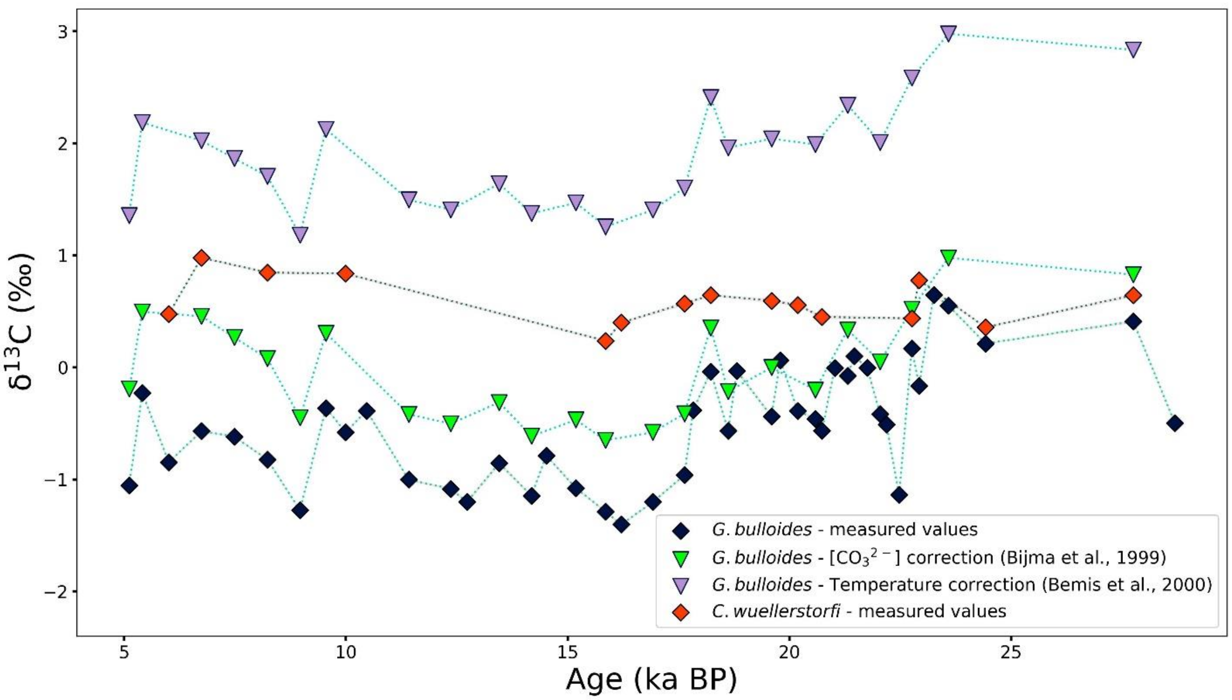

Figure S3. Measured $\delta^{13}C$ values of *G. bulloides* (dark blue diamonds), and *C. wuellerstorfi* red diamonds), and $\delta^{13}C$ values of *G. bulloides* corrected for temperature (purple triangles; Bemis et al., 2000) and [CO_3^{2-}] (green triangles; Bijma et al., 1999) plotted over the past 27 ka BP.

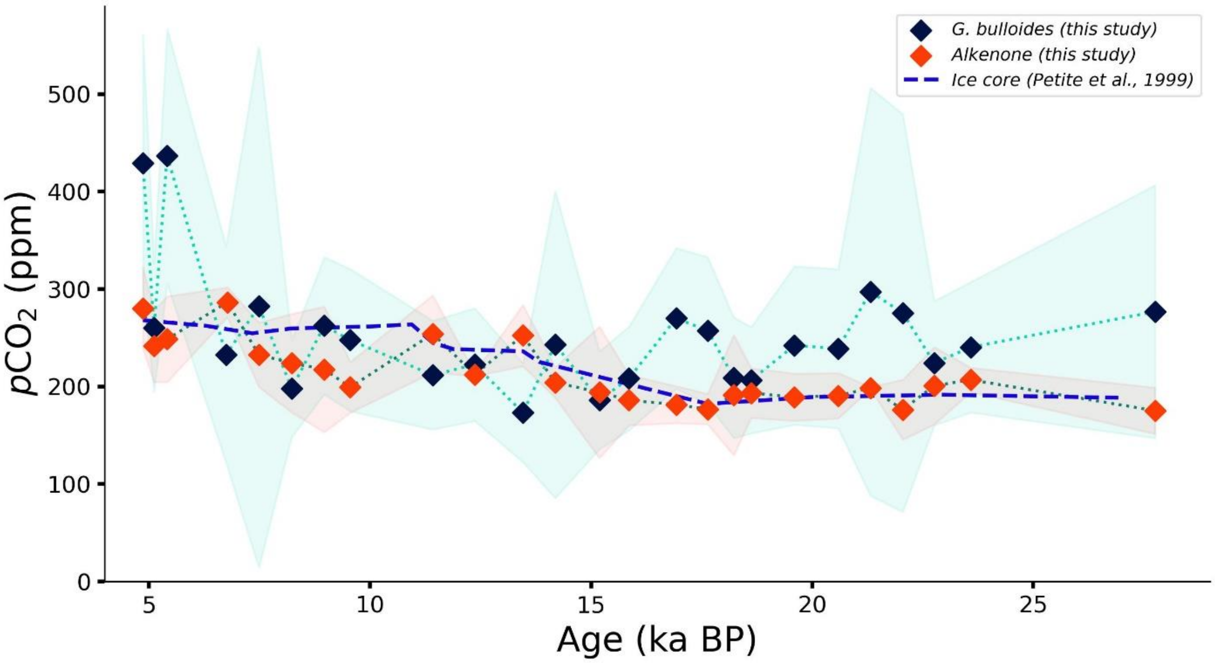

Figure S4. Reconstruction of pCO_2 based on foraminiferal (*G. bulloides*) $\delta^{11}B$ values combined with B/Ca values using the calibration of Krupinski et al. (2017; dark blue diamonds) compared to the pCO_2 reconstruction based on $\delta^{13}C$ of alkenones (red diamonds) and ice core record of pCO_2 (blue dashed line; Petite et al., 1999). Light green and red shaded area represent propagated error for the foraminifera and alkenone based reconstructions, respectively.

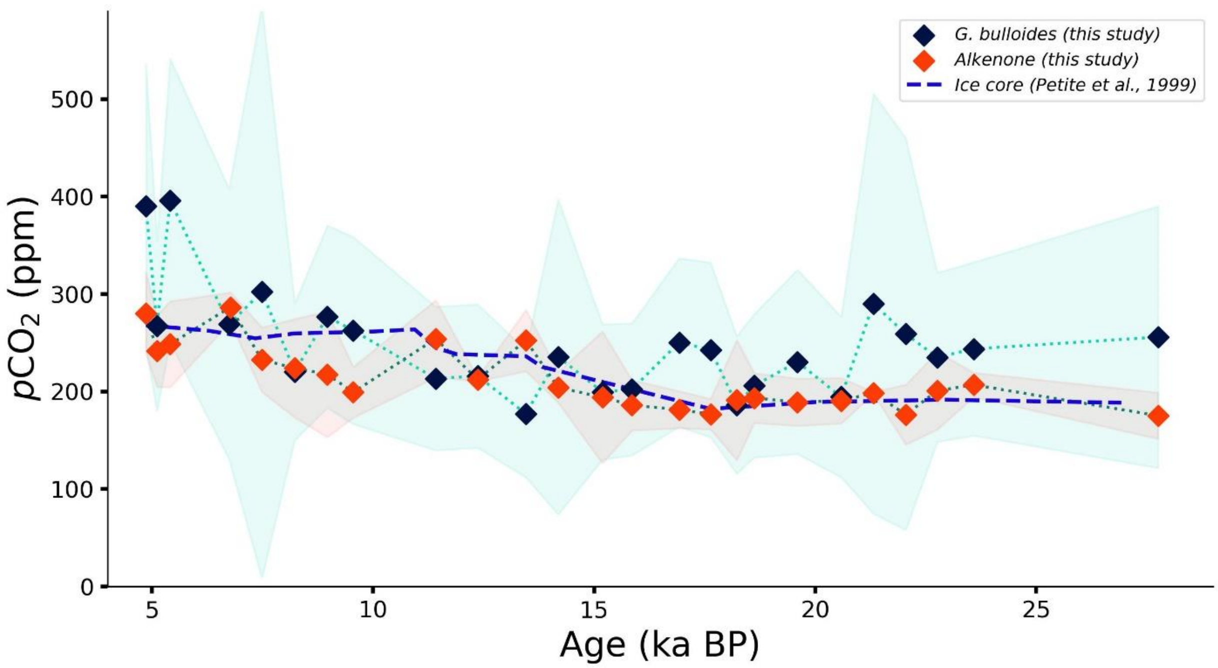

Figure S5. Reconstruction of pCO_2 based on foraminiferal (*G. bulloides*) $\delta^{11}B$ values combined with S/Mg values using the calibration of Karancz et al. (2024; dark blue diamonds) compared to the pCO_2 reconstruction based on $\delta^{13}C$ of alkenones (red diamonds) and ice core record of pCO_2 (blue dashed line; Petite et al., 1999). Light green and red shaded area represent propagated error for the foraminifera and alkenone based reconstructions, respectively.

Text S1: Non-traditional methods for pCO_2 reconstruction

Using the core-top calibration of Krupinski et al. (2017), $[CO_3^{2-}]$ was calculated for each sample based on B/Ca ratios, and subsequently used together with the pH values to reconstruct pCO_2 (Supplementary Figure S4). The difference between the alkenone- and foraminifera-based reconstructions is somewhat reduced when B/Ca is applied instead of total alkalinity. However, because of error propagation, the uncertainty interval increases. Except for two Holocene intervals that show higher values, calculated pCO_2 is generally lowered by 26-79 ppm, making the $\delta^{11}B$ record more similar to the alkenone $\delta^{13}C$ based pCO_2 reconstruction. Still, reconstructed pCO_2 values during the LGM and early deglacial are consistently higher than the atmospheric values.

Application of S/Mg may provide an alternative for B/Ca based reconstructions as this proxy may correct for multiple effects, such as temperature, pH, growth rate, enhancing the predictive power for $[CO_3^{2-}]$ (Karancz et al., 2024). Using $[CO_3^{2-}]$ reconstructed based on S/Mg instead of B/Ca, on average further reduces the difference between the foraminifera and alkenone based pCO_2 values (Supplementary Figure S5).